

Supplemental information: Insights into transducer plane streaming patterns in thin-layered acoustofluidic devices

Junjun Lei,¹ Martyn Hill,¹ and Peter Glynne-Jones¹

¹*Faculty of Engineering and the Environment, University of Southampton, Southampton, SO17 1BJ, UK*

1. Experimental method

The experiments were performed in a transducer-capillary device using a μpiv system (see FIG. 1(a) in the main paper). A function generator (TTi, TG1304 Programmable) drives an RF amplifier (EIN, Model 240L) that drives the transducer, with the signal monitored by an oscilloscope (Agilent Technologies, DOS1102B Digital Storage Oscilloscope). An Olympus BXFM epi-fluorescent microscope with a pixelfly dual-frame CCD camera was used to image the fluid flow. A planar PZT4A transducer (Ferroperm, $3 \times 1.5 \times 1 \text{ mm}^3$) was glued (epoxy, epotek 301, measured glue layer thicknesses $< 10 \text{ }\mu\text{m}$) to a glass capillary of approximately rectangular cross-section, as shown in FIG. 1(b) in the main paper. The glass capillary (Vitricom) had inner dimensions of $0.3 \times 6 \text{ mm}^2$, wall thickness of 0.3 mm , and length of 50 mm . Soldered connections were made between the electrodes and connecting wires. Fluidic connections were made to the capillary via PTFE tubing (ID 1 mm) attached via heat-shrink sleeving.

Green-fluorescent $1 \text{ }\mu\text{m}$ polystyrene tracer beads (Fluoresbrite microspheres, Polysciences Inc.) were used to

characterize the acoustic streaming fields. In each measurement, a fresh supply of beads was flushed into the capillary to ensure a homogeneous bead distribution. Image pairs for the μpiv measurements were captured at measured intervals of about 280 ms and processed using the Matlab based μpiv software, mpiv [1].

2. Derivation of active intensity

Considering a 3D standing wave and a modal travelling wave propagating in the x direction,

$$p_1 = p_{1s} + p_{1t}, \quad (\text{S1a})$$

$$p_{1s} = p_{0s} \cos(k_{xs}x) \cos(k_{ys}y) \sin(k_{zs}z) e^{i\omega t}, \quad (\text{S1b})$$

$$p_{1t} = p_{0t} e^{ik_{xt}x} \cos(k_{yt}y) \sin(k_{zt}z) e^{i(\omega t + \varphi)}, \quad (\text{S1c})$$

where subscripts s and t indicate the standing and travelling wave components (the same below), p_0 is the acoustic pressure amplitudes, k_x , k_y and k_z are the wave numbers in the x , y and z directions, ω is the angular frequency and φ indicates the phase difference between the standing and travelling wave components. From equations S1, we can derive the active intensity fields:

$$I_x = 0.5 \text{Re}[p_1 u_1^*] = \frac{0.5 p_{0t}}{\rho_0 \omega} \sin^2(k_{zt}z) \{-k_{xt} p_{0t} \cos^2(k_{yt}y) - p_{0s} \cos(k_{yt}y) \cos(k_y y) [k_{xt} \cos(k_x x) \cos(k_{xt}x + \varphi) + k_x \sin(k_{xt}x + \varphi) \sin(k_x x)]\}, \quad (\text{S2a})$$

$$I_y = 0.5 \text{Re}[p_1 v_1^*] = \frac{0.5 p_{0t} p_{0s}}{\rho_0 \omega} \sin^2(k_{zt}z) \cos(k_x x) \sin(k_{xt}x + \varphi) \{k_{yt} \cos(k_y y) \sin(k_{yt}y) - k_y \cos(k_{yt}y) \sin(k_y y)\}. \quad (\text{S2b})$$

For the travelling wave mode (t, 0, 1) of interest, where $k_{yt} = 0$, on the driving edges ($z = \pm h/2$), equations S2 can be simplified to

$$I_x = \frac{0.5 p_{0t}}{\rho_0 \omega} \{-k_{xt} p_{0t} - p_{0s} \cos(k_y y) [k_{xt} \cos(k_x x) \cos(k_{xt}x + \varphi) + k_x \sin(k_{xt}x + \varphi) \sin(k_x x)]\}, \quad (\text{S3a})$$

$$I_y = \frac{0.5 p_{0t} p_{0s}}{\rho_0 \omega} \cos(k_x x) \sin(k_{xt}x + \varphi) \{-k_y \sin(k_y y)\}. \quad (\text{S3b})$$

Then, we can find the approximated expression for the maximum active intensity, which follows

$$|I|_{\max} \approx \frac{k_{xt} p_{0t}^2}{2 \rho_0 \omega} \left(1 + \frac{p_{0s}}{p_{0t}}\right). \quad (\text{S4})$$

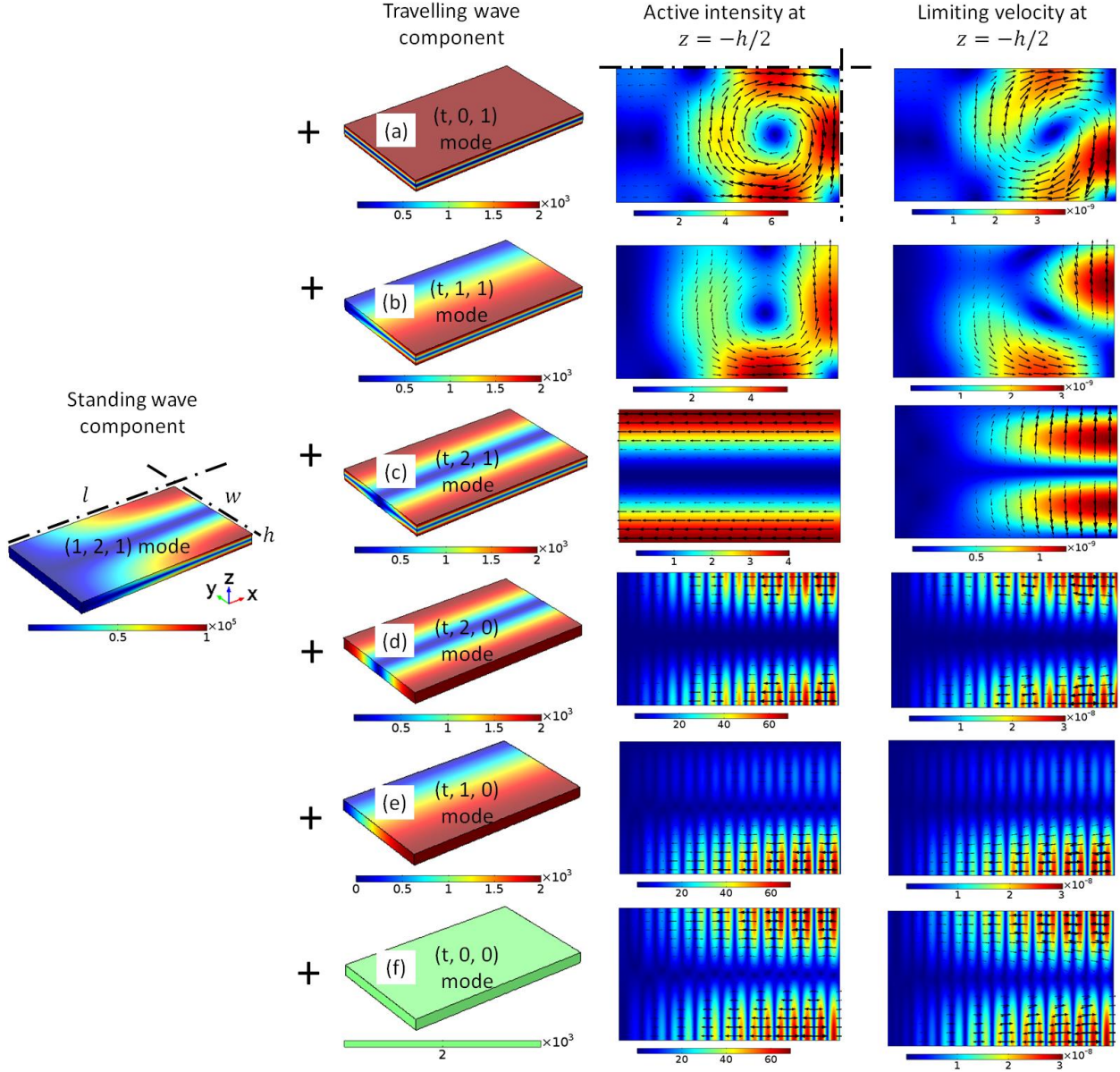


FIG. S1 The active intensity (W/m^2) and limiting velocity (m/s) fields at the driving boundaries for a number of standing and travelling wave components (Pa). The phase difference between the standing and travelling wave components, $\varphi = -\pi/2$.

It was shown that the differences between this expression and the theoretical values are within 5% for $p_{0t} < p_{0s}$ (the condition for the excitation of rotational transducer plane streaming patterns).

3. Additional streaming pattern results

The active intensity and limiting velocity fields under various combination of standing wave and travelling wave modes are presented in FIG. S1. It can be seen that, compared to the travelling mode $(t, 0, 1)$ mode shown in the main manuscript, at the same phase, φ , the travelling wave modes $(t, n, 0)$ do not produce transducer plane streaming, and the higher order mode $(t, 1, 1)$ can produce rotation in the opposite direction.

The pattern shown in FIG. S2 results from an acoustic vortex formed from a superposition of two out-of-phase standing waves. As shown in FIG. S2 (f-g), particles concentrated at the pressure nodes by the acoustic radiation forces are expected to rotate driven by the in-plane acoustic streaming vortices, as described in Ref. [2].

FIG. S3 compares the boundary-driven streaming and Eckart streaming fields for a $(t, 0, 0)$ mode. It is shown that the limiting velocity at the boundary is non-zero for a pure travelling wave field (or when the travelling wave component is dominant), which is in contrast to the no-slip boundary condition for the (typically higher velocity) Eckart streaming. Their reverse streaming velocities in the x -direction reveal that streaming vortices will be generated near the boundaries.

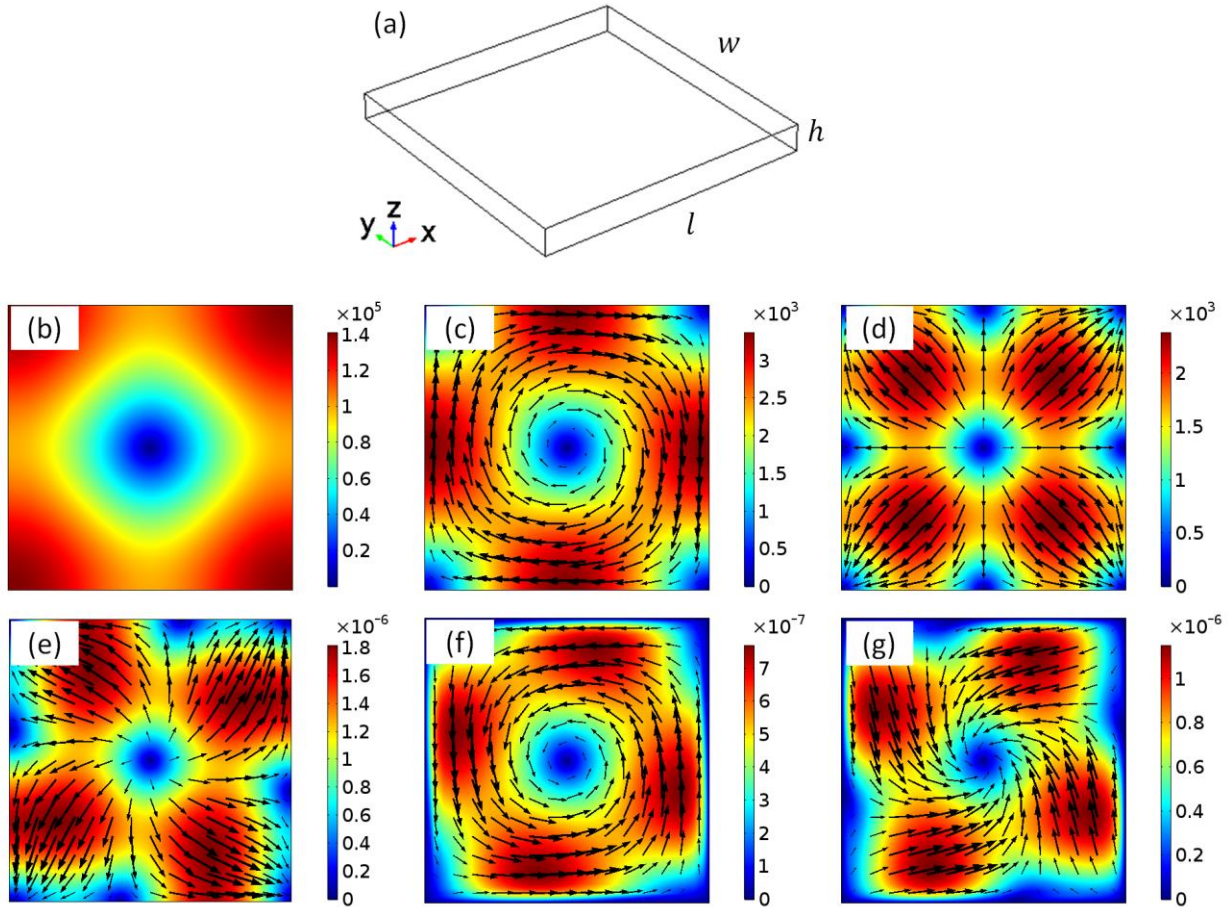


FIG. S2 (a) the model domain; (b) the acoustic pressure magnitudes (Pa); (c) the active intensity field (N/m^2) at the bottom edge ($z = -h/2$); (d) the reactive intensity (W/m^2); (e) the limiting velocity field (m/s) at $z = -h/2$; (f) transducer plane streaming (m/s) at the half-height plane ($z = 0$); and (g) transducer plane streaming at the quarter-height plane ($z = -h/4$). The phase difference between the two orthogonal standing wave fields is $\varphi = \pi/2$. The origin of coordinates is at the centre of the 3D channel shown in (a).

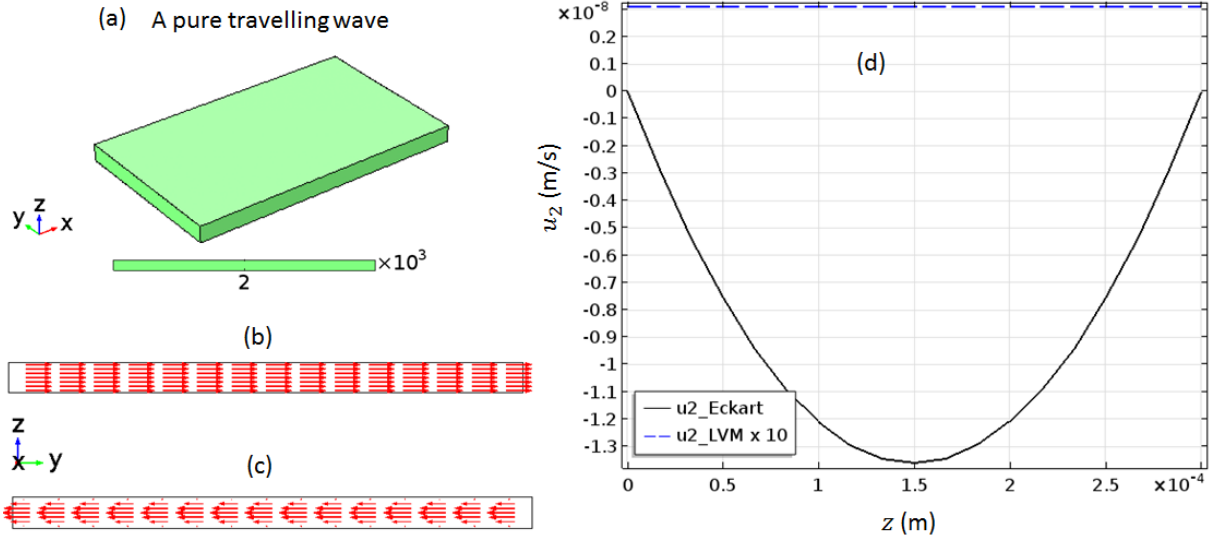


FIG. S3 Comparisons of the modelled streaming fields: (a) A pure travelling wave; (b) boundary-driven streaming; (c) Eckart streaming; and (d) vertical (z) streaming velocity magnitudes, where $u2_Eckart$ and $u2_LVM \times 10$ show the velocity magnitudes of Eckart streaming and boundary-driven streaming, respectively.

References

- [1] mpiv - MATLAB PIV Toolbox, <http://www.oceanwave.jp/software/mpiv/>.
- [2] Z. Y. Hong, J. Zhang, and B. W. Drinkwater, Observation of Orbital Angular Momentum Transfer from Bessel-Shaped Acoustic Vortices to Diphasic Liquid-Microparticle Mixtures, *Phys Rev Lett* **114**, 214301 (2015).